Hydrogen activation by [NiFe]-hydrogenases

Carr, Stephen B.; Evans, Rhiannon M.; Brooke, Emily J.; Wehlin, Sara A. M.; Nomerotskaia, Elena; Sargent, Frank; Armstrong, Fraser A.; Phillips, Simon E. V.

Published in:
Biochemical Society Transactions

DOI:
10.1042/BST20160031

Publication date:
2016

Document Version
Accepted author manuscript

Hydrogen Activation by [NiFe]-hydrogenases

Stephen B. Carr [1*], Rhiannon M. Evans,[2] Emily J. Brooke,[2] Sara A. M. Wehlin,[2] Elena Nomerotskaia,[2] Frank Sargent,[3], Fraser A. Armstrong [2*] and Simon E. V. Phillips [1*]

[1]Research Complex at Harwell, Rutherford Appleton Laboratory, Harwell Oxford, Didcot OX11 0FA, [2]Department of Chemistry, University of Oxford, Oxford OX1 3QR. [3]Division of Molecular Microbiology, School of Life Sciences, University of Dundee, Dundee DD1 5EH. *To whom correspondence should be addressed (emails: Simon.Phillips@rc-harwell.ac.uk, stephen.carr@rc-harwell.ac.uk, fraser.armstrong@chem.ox.ac.uk)

Key words: hydrogenase, hydrogen splitting, frustrated Lewis pair, protein film electrochemistry, crystal structure, mutagenesis

Abbreviations: Hyd-1 – *E.coli* Hydrogenase-1; FLP – frustrated Lewis pair; PFE – protein film electrochemistry; r.m.s. – root mean square; PDB – Protein Data Bank.

Abstract

Hydrogenase-1 (Hyd-1) from *E. coli* is a membrane-bound enzyme that catalyzes the reversible oxidation of molecular H_2. The active site contains one Fe and one Ni atom and several conserved amino acids including an arginine (509), which interacts with two conserved aspartate residues (118 and 574) forming an outer shell canopy over the active site, There is also a highly conserved glutamate (28) positioned on the opposite side of the active site to the canopy. The mechanism of hydrogen activation has been dissected by site-directed mutagenesis to identify the catalytic base responsible for

splitting molecular hydrogen and possible proton transfer pathways to/from the active site. Previous reported attempts to mutate residues in the canopy were unsuccessful, leading to an assumption of a purely structural role. Recent discoveries, however, suggest a catalytic requirement for example, replacing the arginine with lysine (R509K) leaves the structure virtually unchanged, but catalytic activity falls by more than 100-fold. Variants containing amino acid substitutions at either, or both, aspartates retain significant activity. We now propose a new mechanism: heterolytic H_2 cleavage is *via* a mechanism akin to that of a frustrated Lewis pair (FLP), where H_2 is polarized by simultaneous binding to the metal(s) (the acid) and a nitrogen from Arg509 (the base).

Introduction

Hydrogenases are metalloenzymes that catalyse the conversion of molecular H_2 to protons and electrons, and the reverse reaction to regenerate H_2 (reviewed in [1]). They are found in the periplasm or cytoplasm of bacteria, archaea and some eukaryotes, either as soluble enzymes or in membrane-bound form, with various functions, including provision of energy by oxidation of H_2, balancing the redox potential of the cell, establishing transmembrane gradients, sensing and signalling. There are three classes, with [NiFe], [FeFe] or [Fe] metal centres respectively, and the chemical mechanism of efficient hydrogen cleavage or generation by these enymes is of particular interest because, unlike man-made catalysts, they do not require a noble metal such as Pt.

There are three types of [NiFe] hydrogenases: Membrane Bound, Regulatory and Soluble. The metal ions are coordinated by two bridging sulphurs from protein cysteine side-chains, the Ni by two further ‘terminal’ cysteine sulphurs, and the Fe by two inorganic cyanides and

one carbonyl ligand. A third bridging site is open for binding of substrate H_2 and other small ligands, such as hydroxide (see later). The reaction cycle involves complex proton-coupled electron transfers, with the resulting electrons produced transferred from the metal centre to a string of FeS clusters leading to the protein surface [2]. During the reaction cycle both Ni and Fe are initially in formal oxidation state II, with Ni passing through Ni(II)–H^- (Ni-R, a hydrido species) Ni(III) –H^- (Ni-C, also a hydrido species), and probably Ni(I) (Ni-L, in which hydride has migrated as H^+) before returning to the starting point II (Ni-SI). Binding of H_2 to a metal increases its acidity, facilitating heterolytic cleavage via abstraction of H^+ by a nearby base and leaving a bridging H^- at the metal centre. [NiFe] hydrogenases are susceptible to aerobic oxidation, forming NiIII species that require reductive activation (termed 'Ready' and 'Unready' states, respectively, in order of ease of reductive re-activation). A subclass referred to as 'O_2-tolerant' [NiFe] hydrogenases are able to sustain H_2 oxidation in the presence of O_2, owing to their exclusive formation of the Ready state (also known as Ni-B) which is rapidly re-activated [3].

Hydrogenase structure and activity.

Several crystal structures have been determined for bacterial [NiFe] hydrogenases, showing similar folds, which reflect significant sequence conservation, and very similar active sites [1]. Figure 1 shows the structure of (Hyd-1), a membrane-bound [NiFe] hydrogenase that is tolerant to O_2 exposure [4]. It is a heterotetramer, consisting of two identical small subunits and two identical large subunits. The small subunits anchor the enzyme to the periplasmic side of the cytoplasmic membrane via a C-terminal single-pass transmembrane (TM) helix, and contain three FeS clusters which serve to transfer electrons from the active site to an associated membrane bound Cytochrome *b*. The large subunits harbour the [NiFe] centre and likely entry channels for H_2 and exit pathways for H^+.

Structural analysis of various [NiFe] hydrogenases reveal a long channel extending from the surface of the enzyme to the active site that has been proposed to be the entry route for H_2. The channel can bind Xenon [5] or Krypton [6] in crystals demonstrating an affinity for gas molecules. Site directed mutagenesis provides further evidence that H_2 enters via this channel, for example, double mutant Val74Ile, Leu122Phe of *D. fructosovorans* (Val78 and Leu126 in *E. coli*) hydrogenase constricts the end of the channel closest to the active site. This does not affect the turnover rate of the variant enzyme, but leads to a five-fold increase in K_M [7] with respect to H_2, suggesting gas molecules have reduced access to the active site. Conversely, increasing the size of gas channels in an oxygen tolerant regulatory hydrogenase from *R. eutropha* produces an enzyme that is sensitive to inhibition by oxygen, because oxygen is no longer prevented from reaching the active site [8].

Once hydrogen molecules are split the resultant protons are likely to travel through the enzyme via a Grotthuss-like mechanism, with H^+ being transferred between charged or polar groups within hydrogen bonding distance of each other. Replacement of strictly conserved Glu25 of *D. fructosovorans* (Glu28 in *E. coli*), positioned next to the [NiFe] cluster, with glutamine produces an enzyme capable of splitting/recombining H_2, but incapable of turnover. This suggests Glu28 is an entry point into a proton transfer pathway, since proton transport is a requirement for enzymatic turnover, but not for substrate cleavage [9]. Additionally, structural analysis of *D. vulgaris* hydrogenase has identified three possible proton transfer routes starting from this conserved glutamate [10]. A second proton transfer pathway was identified by mutagenesis of a highly-conserved, histidine-rich motif observed in many membrane bound hydrogenases [11]. Mutagenesis of His104 from *D. gigas* hydrogenase (His119 in *E. coli*) produced an enzyme with a significantly impaired activity and computational analysis identified a possible route for proton transfer independent of Glu28 but including the highly conserved Asp118 (see below) and His119 [11] .

The active site also contains a strictly conserved arginine, Arg509 in Hyd-1, above the metal centre and proposed substrate binding site, with one Nη atom only 4.5 Å from the Ni ion (Figure 2). The very close proximity to the electropositive metal centre, and strict sequence conservation implies a functional importance for this arginine, but it has been largely ignored as a candidate for the active site base owing to the typically high pK_a of arginine residues. Arg509 also interacts with two highly conserved aspartates, Asp118 and Asp574, to form a conserved canopy above the active site. The conservation of the arginine had been attributed to a role in stabilization of the structure, including a proposed hydrogen bond to one of the Fe cyanide ligands [12, 13], although the geometry of this hydrogen bond is not favourable. The functional role of the arginine has not, however, been investigated by site-directed mutagenesis, although there were two unsuccessful attempts to replace the arginine with alternative side-chains in enzymes from *Thiocapsa roseopersicina* [11] and *Desulfovibrio fructosovorans* [14], which did not lead to production of mature enzyme.

Proposals for the catalytic mechanism have previously centred on the suggestion that the base might be a terminal cysteine ligand coordinated to the Ni ion, Cys574 in Hyd-1(Figure 2), adjacent to the substrate binding site [15, 16]. A recent 0.89 Å resolution crystal structure for the [NiFe] hydrogenase from *Desulfovibrio vulgaris*, specifically in the active reduced Ni-R form, gave electron density maps of outstanding quality where many hydrogen atoms were clearly visible [10]. The structure was consistent with the presence of a bound hydride ion bridging the metals, with some difference electron density on the sulphur atom for Cys574, which the authors interpreted as the H^+ product of cleavage, although the geometry was unusual.

Structure and activity of *E. coli* Hyd-1 canopy variants

Recently, a combination of site-directed mutagenesis, electrochemistry and X-ray crystallography has been used to investigate whether the conserved, "canopy-forming"

residues in Hyd-1 have a role in activation of H_2 [17]. Mutations Arg509Lys, Asp574Asn, Asp118Ala and Asp118Asn/Asp574Asn (double substitution) were introduced and their hydrogen oxidation activities measured as 0.8%, 83%, 26% and 20% of the H_2 oxidation activity of native Hyd-1 (Figure 2). Additionally, protein-film electrochemistry (PFE) showed all mutants had similar potentials for the onset of catalytic H_2 oxidation, a property mainly dependent on the FeS clusters [18, 19]. The characteristic shape of the curve for native enzyme was retained for Arg509Lys, while the other variants showed negative shifts in the high-potential threshold indicating some stabilization of the 'resting' Ni^{III}-OH state [20, 21]. High resolution X-ray crystal structures showed the mutations had minimal effect on the structure of the protein, and the main-chain atoms of the refined atomic models of all variants could be superimposed on those of the native enzyme with root mean square (r.m.s.) deviations in the range 0.12-0.16Å. The local conformations of the mutated canopy residues, 509, 118 and 574, had even smaller main-chain r.m.s. deviations of 0.10-0.12Å. The cysteine residues coordinating the metal ion were also unaffected by the incorporated amino acid substitutions, although Cys79 showed evidence of partial oxidation to sulphenic acid (Figure 2) as a result of exposure to oxygen during purification [22]. The positions and occupancies of the Ni and Fe ions showed no significant changes between the variants, as judged by *Fo-Fo* difference electron density maps, which are particularly sensitive to small changes in electron-dense atoms. In all cases a small ligand was observed bridging the metal ions, and was assigned as a hydroxyl ion [23].

The side-chain conformations in the variants showed only small differences. The conformation of Lys509 is very similar to Arg509, with small adjustments in side-chain torsion angles to maintain the hydrogen bond with Asp118. The position of N_ζ, superimposes closely on that of the corresponding Arg509 $N\eta$, at a similar distance of 4.4Å above the Ni ion (Figure 2). The smaller side chain allows space for one additional ordered water

molecule near the canopy residues [17]. The entire active site structure of Arg509Lys shows minimal disturbance from that of the native enzyme, indicating that structural change is not the origin of the considerable reduction in catalytic activity. In Asp118Ala the smaller side chain does not result in additional water molecules, but Arg509 moves slightly closer to the metal ions as a consequence of the loss of the hydrogen bonds to Asp118. The replacement of Asp574 with asparagine results in only a small rotation of the side-chain, and one new hydrogen bond between its $N_{\delta}2$ and $O_{\delta}1$of Asp118. In the double substitution variant, where both aspartate residues are replaced by asparagine, the side-chain of Asn118 rotates away from Arg509 to relieve the unfavourable contact between their terminal NH groups, but retains the hydrogen bond from its $O_{\delta}1$.

Discussion

Site directed mutagenesis in combination with structural and spectroscopic analysis have been invaluable in understanding many aspects of hydrogenase function: including how hydrogen enters to the active site, how protons are transported away after turnover, and most recently a new view as to how activation of H_2 facilitates cleavage. The replacement of Arg509 by lysine results in over 100-fold reduction in catalytic activity, despite a lack of structural change, which is remarkable given the significant alterations to the hydrogen bonding network at the active site that the different variants introduce. The significant decrease in hydrogen oxidation activity overturns the previous assumption that the role of Arg509 is simply structural and provides powerful evidence for the direct involvement of the guanidinium group of Arg509 in catalysis. It had previously been suggested that the catalytic base for H_2 cleavage was one of the cysteine ligands to the Ni ion (Cys579 in Hyd-1), but a coordinated thiolate-S is expected to be a weak base [24]. On the other hand, the guanidinium group of Arg509 is a very strong base, capable of abstracting a proton if it was itself deprotonated. Arginine side-chains normally have a pK_a of 12 or more, but enzymes

often tune the properties of side-chains by creating specific environments and the use of arginine as a catalytic base is not unprecedented. For example, it is accepted in the mechanisms of fumarate reductase and L-aspartate oxidase, as well as a proposed role in photosystem II [25, 26, 27]. The question that needs to be addressed is how Hyd-1 Arg509 can be deprotonated in order to act as the necessary base. Hyd-1, with other [NiFe] hydrogenases, is a reversible electrocatalyst, so that each step of the catalytic cycle should be reversible according to the appropriate potentials. In addition, a hydrido ligand bound to the reduced metal centre would be an exceptionally strong base [28], while a bound H_2 would be a weak acid. The structure of the Ni-R form, with a bound hydride ion was established by the high resolution crystal structure discussed above [10] and the active site is shown schematically in Figure 3. One Nη atom of Arg 509 is positioned close to the metal centre with favourable geometry for the strongly basic hydride ligand to deprotonate it and form H_2. Consequently, the reverse reaction, heterolytic cleavage of H_2 must also be possible. The reaction can be driven in either direction depending on the electrochemical potential, i.e. the supply or withdrawal of electrons. The heterolytic activation of hydrogen by arginine and the metal centre is similar to that of a frustrated Lewis pair (FLP) [29] where a strong Lewis acid and strong Lewis base are placed in close proximity, but are sterically prevented from reacting with each other. Such an arrangement allows the Lewis acid and base to act cooperatively to activate small molecules such as H_2. In the active site of hydrogenases binding of hydrogen to the metal centre polarises the molecule and greatly increases its acidity facilitating the abstraction of a proton by the (Lewis) base. It has been proposed, that the catalytic base in [NiFe] hydrogenases is Arg509 in Hyd-1 [17], and the corresponding residue in other homologues. Interestingly, a related mechanism is proposed for [FeFe] hydrogenases, where an unusual bridging ligand places a pendant nitrogen over the substrate binding site, that is essential for catalysis [30]. In addition, some active synthetic

hydrogenase analogues also have a pendant base over a redox-active metal ion [31]. There is now a convergence of [NiFe] and [FeFe] hydrogenases, with the synthetic analogues, towards an FLP mechanism for splitting hydrogen.

Accession codes

The coordinates and structure factors are available from the protein data bank with accession codes 4UE3 (R509K), 5A4F (D118A), 5A4I (D574N), 5A4M (deltaTM) and 5ADU (D118N/D574N).

Acknowledgements

We thank Diamond Light Source for beam time proposal mx9306 and the staff of beamlines i02, i04 and i04-1 for their assistance during data collection.

Funding

This work was supported by the UK Biological and Biotechnology Sciences Research Council, Grants BB/I022309-1 and BB/L009722/1 to F.A.A, BB/L008521/1 to F.S, and from the UK Medical Research Council G0901251 to S.E.V.P and S.B.C. A studentship for E.J.B was supported by grants from Global Innovation Initiative and the UK Engineering and Physical Sciences Research Council. F.A.A. is a Royal Society Wolfson Research Merit Award holder.

References

1. Lubitz, W., Ogata, H., Rüdiger, O. & Reijerse, E. (2014) Hydrogenases. Chem. Rev. **114**, 4081–4148.

2. Flanagan, L.A. & Parkin, A. (2016) Electrochemical insights into the mechanism of NiFe membrane bound hydrogenases. Biochem. Soc. Trans. **44**, 315-328.

3. Evans, R.M. *et al.* (2013) Principles of sustained enzymatic hydrogen oxidation in the presence of oxygen—the crucial influence of high potential Fe-S clusters in the electron relay of [NiFe]-hydrogenases. J. Am. Chem. Soc. **135**, 2694–2707.

4. Volbeda, A. *et al.* (2012) X-ray crystallographic and computational studies of the O2-tolerant [NiFe]-hydrogenase 1 from *Escherichia coli*. Proc. Natl. Acad. Sci. USA **109**, 5305–5310.

5. Montet, Y. *et al.* (1997) Gas access to the active site of NiFe hydrogenases probed by X-ray crystallography and molecular dynamics. *Nat. Struct. Mol. Biol.* **4**, 523-526.

6. Leroux, F. *et al.* (2008) Experimental approaches to kinetics of gas diffusion in hydrogenase. Proc. Natl. Acad. Sci. USA **105**, 11188–11193.

7. Kalms, J. *et al.* (2016) Krypton Derivatization of an O_2-Tolerant Membrane-Bound [NiFe] Hydrogenase Reveals a Hydrophobic Tunnel Network for Gas Transport. *Angewandte Chemie Int. Ed.* In Press doi10.1002/anie.201508976

8. Buhrke, T., Lenz, O., Krauss, N. & Friedrich, B (2005) Oxygen tolerance of the H_2-sensing [NiFe] hydrogenase from *Ralstonia eutropha* H16 is based on limited access of oxygen to the active site. *J. Biol. Chem.* **280**, 23791-23796.

9. Dementin S. *et al.* (2004) A Glutamate is the essential proton transfer gate during the catalytic cycle of the [NiFe] hydrogenase. *J. Biol. Chem.* **279**, 10508-10513.

10. Ogata, H., Nishikawa, K. & Lubitz, W. (2015) Hydrogens detected by subatomic resolution protein crystallography in a [NiFe] hydrogenase. Nature **520**, 571–574.

11. Szőri-Dorogházi, E. *et al.* (2012) Analyses of the large subunit histidine-rich motif expose an alternative proton transfer pathway in [NiFe] hydrogenases. PLoS One **7**, e34666.

12. Volbeda, A. *et al.* (1996) Structure of the [NiFe] hydrogenase active site: evidence for biologically uncommon Fe ligands. J. Am. Chem. Soc. **118**, 12989–12996.

13. de Lacey, A.L. *et al.* (1997) Infrared-spectroelectrochemical characterization of the [NiFe] hydrogenase of *Desulfovibrio gigas*. J. Am. Chem. Soc. **119**, 7181–7189.

14. deLacey, A.L., Fernandez, V.M., Rousset, M., Cavazza, C. & Hatchikian, E.C. (2003) Spectroscopic and kinetic characterization of active site mutants of *Desulfovibrio fructosovorans* Ni-Fe hydrogenase. J. Biol. Inorg. Chem. **8**, 129–134.

15. Amara, P., Volbeda, A., Fonticilla-Camps, J.C. & Field, M.J. (1999) A hybrid density functional theory/molecular mechanics study of nickel-iron hydrogenase: investigation of the active redox states. *J. Am. Chem. Soc.* **121**, 4468-4477.

16. Ogata, H. *et al.* (2002) Structural studies of the carbon monoxide complex of [NiFe] hydrogenase from Desulfovibrio vulgaris Miyazaki F: suggestion for the initial activation site for dihydrogen. *J. Am. Chem. Soc.* **124**, 11628-11635

17. Evans, R.M., Brooke, E.J., Wehlin, S.A.M., Nomerotskaia, E., Sargent, F., Carr, S.B., Phillips, S.E.V. and Armstrong, F.A. (2016) Mechanism of hydrogen activation by [NiFe] hydrogenases. Nature Chem. Biol. **12**, 46-50.

18. Hexter, S.V., Grey, F., Happe, T., Climent, V. & Armstrong, F.A. (2012) Electrocatalytic mechanism of reversible hydrogen cycling by enzymes and distinctions between the major classes of hydrogenases. Proc. Natl. Acad. Sci. *USA* **109**, 11516–11521.

19. Murphy, B.J., Sargent, F. & Armstrong, F.A. (2014)Transforming an oxygen-tolerant NiFe uptake hydrogenase into a proficient, reversible hydrogen producer. Energy Environ. Sci. **7**, 1426–1433.

20. Armstrong, F.A. (2009) Dynamic electrochemical experiments on hydrogenases. Photosynth. Res. **102**, 541–550.

21. Armstrong, F.A. *et al.* (2009) Dynamic electrochemical investigations of hydrogen oxidation and production by enzymes and implications for future technology. Chem. Soc. Rev. **38**, 36–51.

22. Volbeda, A. *et al.* (2015) Crystallographic studies of [NiFe]-hydrogenase mutants: towards consensus structures for the elusive unready oxidized states. J. Biol. Inorg. Chem. **20**, 11–22.

23. Fontecilla-Camps, J.C., Volbeda, A., Cavazza, C. & Nicolet, Y. (2007) Structure/function relationships of [NiFe]- and [FeFe]-hydrogenases. Chem. Rev. **107**, 4273–4303.

24. Simmons, T.R., Berggren, G., Bacchi, M., Fontecave, M. & Artero, V. (2014) Mimicking hydrogenases: from biomimetics to artificial enzymes. Coord. Chem. Rev. **270**–**271**, 127–150.

25. Guillén Schlippe, Y.V. & Hedstrom, L. (2005) A twisted base? The role of arginine in enzyme-catalyzed proton abstractions. Arch. Biochem. Biophys. **433**, 266–278.

26. Pankhurst, K.L. *et al.* (2006) A proton delivery pathway in the soluble fumarate reductase from *Shewanella frigidimarina*. J. Biol. Chem. **281**, 20589–20597.

27. Tedeschi, G. *et al.* (2001) Probing the active site of L-aspartate oxidase by site-directed mutagenesis: role of basic residues in fumarate reduction. Biochemistry **40**, 4738–4744.

28. Morris, R.H. (2014)Estimating the acidity of transition metal hydride and dihydrogen complexes by adding ligand acidity constants. J. Am. Chem. Soc. **136**, 1948–1959.

29. Stephan, D.W. & Erker, G. (2010) Frustrated Lewis pairs: metal-free hydrogen activation and more. Angew. Chem. Int. Ed. Engl. **49**, 46–76.

30. Berggren, G. *et al.* (2013) Biomimetic assembly and activation of [FeFe]-hydrogenases. Nature **499**, 66–69.

31. Ginovska-Pangovska, B., Dutta, A., Reback, M.L., Linehan, J.C. & Shaw, W.J. (2014) Beyond the Active Site: The Impact of the Outer Coordination Sphere on electrocatalysts for Hydrogen Production and Oxidation. *Accounts of Chemical Research*, **47**, 2621-2630.

Figure Legends

Figure 1

The structure of deltaTM Hyd-1 (PDB: 5A4M) showing the overall fold and functionally important prosthetic groups. The two small subunits are shown in different shades of blue, while the two large subunits are shown in yellow and bronze. The [NiFe] centres and FeS clusters are shown as spheres.

Figure 2

Active site structures and catalytic activities for native Hyd-1 and variants investigated in this research. The histogram shows average turnover rate (s^{-1}) for each enzyme, with error bars indicating the standard error of the mean of at least twenty repeats with at least two different preparations of each enzyme. On the left is the active site of native (deltaTM) Hyd-1 (PDB: 5A4M) and the right Arg509Lys (PDB: 4UE3). The Ni atom (green), Fe atom (bronze) and the O atom of the bridging hydroxide (red) are all shown as spheres. Some oxidation of C79

to sulfenic acid was observed at the active site of each variant (not shown). The closest distance between the Ni and N atom of residue 509 (dashed lines) is also indicated. Residues His 119 is shown on the WT structure and Glu28 on Arg509Lys to indicate the position of the proton transfer pathways relative to the [NiFe]-centre modified from [17] with permission

Figure 3

Proposal for the H_2 activation step in [NiFe] hydrogenases using suspended arginine as a general base, as in a frustrated Lewis pair mechanism. Hydrogen is polarized between the metal (acid) and deprotonated guanidine (base) of Arg509, oxidizing H_2 and forming the Ni-R species (left). The hydridic Ni-R species deprotonates the guanidinum headgroup of Arg509, forming molecular hydrogen. Modified from [17] with permission.

Figure 1

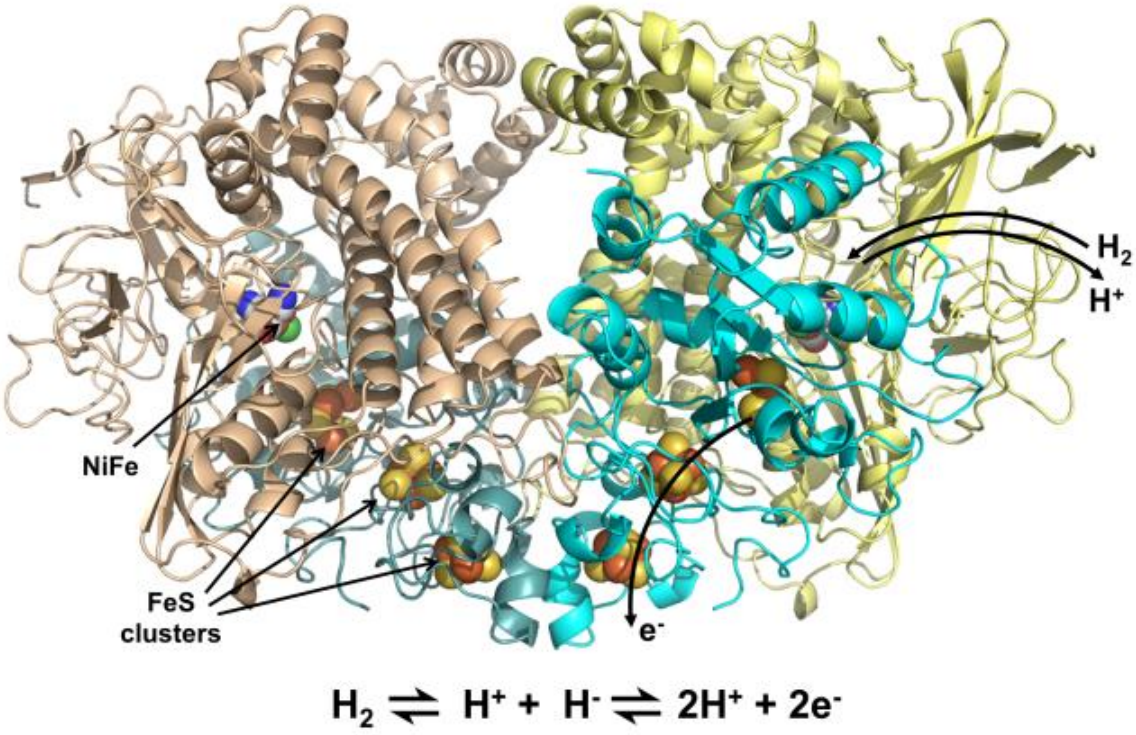

Figure 2

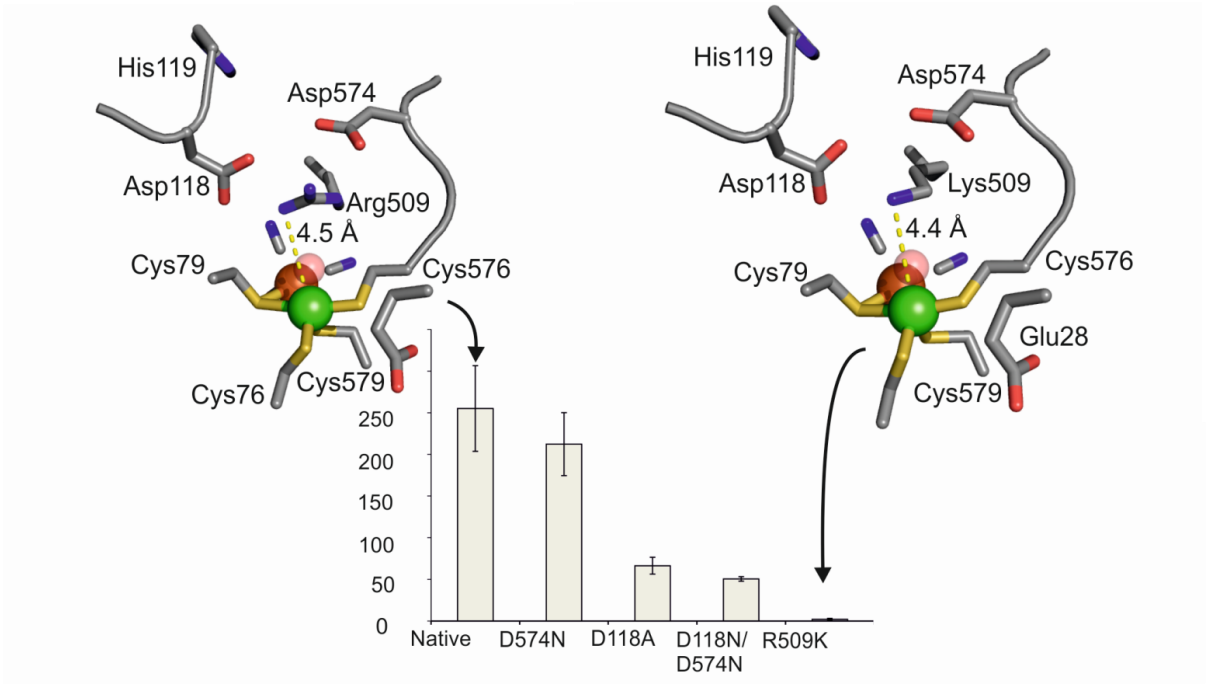
His119
Asp574
Asp118
Arg509
4.5 Å
Cys79
Cys576
Cys76
Cys579
His119
Asp574
Asp118
Lys509
4.4 Å
Cys79
Cys576
Glu28
Cys579
250
200
150
100
50
0
Native
D574N
D118A
D118N/
D574N
R509K

Figure 3